INTERAGENCY FUNDED QUANTUM WELL INFRARED PHOTODETECTOR (QWIP) RESEARCH AND DEVELOPMENT AT JET PROPULSION LABORATORY FOR NASA AND DEFENSE APPLICATIONS

S. D. Gunapala, S. V. Bandara, J. K. Liu, M. J. McKelvey, E. M. Luong, J. M. Mumolo, N. Tran, and W. Hong

Center for Space Microelectronics Technology, Jet Propulsion Laboratory,
California Institute of Technology, Pasadena, California

ABSTRACT

NASA, commercial, medical, and defense applications such as Earth observation systems, astronomy, weather monitoring, thermal mapping, thermography, missile tracking, and night vision aids, etc. require high performance large format long-wavelength infrared (LWIR) detector arrays in the range of 8-16μm. Thus, NASA and Ballistic Missile Defense Organization (BMDO) have devoted a significant effort in developing highly sensitive **infrared (IR) detectors** and large format focal plane arrays based on novel "artificial" low "effective" band-gap semiconductor material systems such as GaAs/AlGaAs. As a result, Jet Propulsion Laboratory (JPL) has started to investigate **GaAs/AlGaAs** based **multi-quantum wells (MQWs)** for IR radiation detection. Fundamental studies of quantum wells, materials research and development of light coupling schemes to **Quantum Well Infrared Photodetectors (QWIPs)** at JPL was funded by NASA Office of Space Science. Development of large format focal plane arrays based on QWIPs was funded by BMDO's Office of Innovative Science and Technology. Optimization of the detector design, light coupling schemes, large format focal plane array fabrication and packaging has culminated in the realization of **portable infrared cameras** with a large (256x256 pixel) **focal plane array** of QWIPs, and the demonstration of TV format (i.e., 640x486) QWIP camera which can see at 8.5 μm, holding forth great promise for myriad applications in the 6-20 μm wavelength range. In this paper we discuss our experience of how effective partnering of government agencies and industries could help develop needed technology for NASA's Space Science and Earth Science Programs. Also, we discuss some applications of this technology and some public outreach activities.

INTRODUCTION

Visible light spanning the wavelength range from blue (~ 0.4 μm) to red (~ 0.7 μm) is a tiny slice of the electromagnetic spectrum. While an enormous wealth of scientific information can be and is obtained through imaging and spectroscopy of objects in visible light, the invisible portion of the spectrum can be harvested to yield both more detailed and new information. Objects that are invisible to the human eye may be visible at other wavelengths. For instance, an object at room temperature (~ 300 K) and in complete darkness may be perfectly invisible to the human eye; but its temperature will make it glow in the infrared (at wavelengths longer than the 0.7 μm wavelength of red light), shining brightest at an infrared (IR) wavelength of around 8.5 μm. A camera which can see 8.5 μm light and convert an 8.5 μm image to a visible black-and-white image on a standard TV monitor or camcorder viewfinder may make the invisible scene spring to life. Temperature and emissivity variations in the dark scene translate to contrast in the gray scale of the black-and-white image, rendering objects and their motion visible. This is the basis of a night-vision (or IR) camera.

While the invisible portion of the electromagnetic spectrum includes gamma rays, X rays, and ultraviolet rays beyond the blue end of the visible spectrum, and infrared rays (spanning a wide wavelength swath from ~ 0.7 μm to ~ 1 mm) and microwaves beyond the red end, light detectors operating in the 3-18 μm wavelength range hold a special significance. Potential applications at these wavelengths range from the mundane to the sublime. As stated earlier, room temperature objects glow brightest in this wavelength range. Detectors with the sharpest eyes for light at these wavelengths are ideal for a variety of ground- and space-based applications such as night vision, early warning systems, navigation, flight control systems, weather monitoring, security and surveillance, etc. In addition, they can be used to monitor and measure pollution, relative humidity profiles, and the distribution of different gases (e.g., O_3, CO, N_2O, etc.) in the atmosphere. This is due to the fact that most of the absorption lines of gas molecules lie in this IR spectral region. The Earth's atmosphere is opaque to most of the infrared; of its few transparent windows, the 8-12 μm is one of the clearest. Cameras operating in this wavelength range and used in ground-based telescopes will be able to see through the Earth's atmosphere, image distant stars and galaxies (including those invisible to telescopes equipped with normal visible eyes), and help in the search for cold objects such as planets orbiting nearby stars. IR detectors operating in the 3-20 μm wavelength range thus find many applications in NASA, medicine, commerce, and defense[1,2].

Since the mid-fifties many government agencies such as NASA, Department of Defense (DOD), etc. have spent a substantial amount of money in the development of novel IR detectors. The most common photon detectors are based on the principle of interband absorption in narrow bandgap semiconductors like InSb, $Hg_xCd_{1-x}Te$, etc. IR radiation is absorbed by the photosensitive material when an incoming photon has sufficient energy E (= hv) to photoexcite an electron across the energy bandgap from the valence band to the conduction band. This process is equivalent to providing enough energy to free a valence electron (so called, because it is loosely bound to the atoms in the semiconductor crystal) and make it available for the conduction of electric current. Such a photoexcited electron is called a photoelectron. Photons with energies less than the bandgap energy are not absorbed; they simply pass through the semiconductor. The bandgap energy therefore defines the low energy (or long wavelength cut-off) absorption edge of the detector. Applying a voltage bias across the detector creates an electric field that sweeps out both photocarriers producing a photocurrent in the external circuit. Such a detector need not be doped and is called an intrinsic detector. Large two-dimensional arrays of InSb (512x512 pixels) and $Hg_{1-x}Cd_xTe$ (128x128 pixels) detectors have already been demonstrated up to cut-off wavelengths of 5 μm and 11 μm respectively. The move to larger pixel arrays is driven by the need for greater scene resolution. Since the bandgap of InSb is fixed, InSb photodetectors cannot detect light at wavelengths longer than 5 μm.

Longer wavelengths can be accessed by narrowing the bandgap of $Hg_{1-x}Cd_xTe$ by changing its alloy composition x. However, such narrow bandgap materials are more difficult to grow and process into devices, reducing the yield and increasing the cost of the arrays . These difficulties motivate the exploration of *artificial* low *effective* bandgap structures built from wide bandgap semiconductors such as GaAs (see Fig.1) which are far easier to grow and process into devices. A low effective bandgap can be created in a quantum well, which resides entirely in either the conduction band or the valence band of a wide bandgap semiconductor like GaAs. Such a GaAs-based Quantum Well Infrared Photodetector (QWIP) then benefits from the highly mature GaAs growth and processing technologies, a benefit that becomes increasingly critical at the longer wavelengths where narrow bandgap materials become more tough to work with. As a result, in 1991 Jet Propulsion Laboratory (JPL) started to investigate GaAs/AlGaAs based MQW structures for IR radiation detection. Fundamental studies of MQW structures, materials research, and development of light coupling schemes to Quantum Well Infrared Photodetectors (QWIPs) at JPL were funded by NASA Office of Space Science. Development of large format focal plane arrays (FPAs) based on QWIPs was funded by BMDO Office of Innovative Science and Technology. As a consequence, we have demonstrated the first hand-held and palm-size 256x256 LWIR imaging cameras, and TV format (i.e., 640x486) LWIR imaging camera based on GaAs/AlGaAs QWIPs, broad-band QWIPs, dualband QWIPs, high-performance QWIPs for NASA's astronomy and DOD's strategic applications.

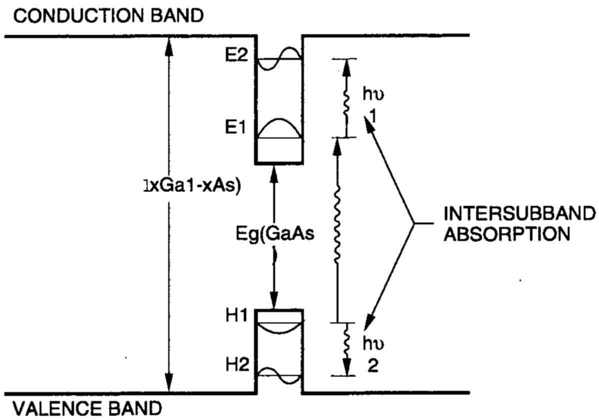

Figure 1 Schematic band diagram of a quantum well. Intersubband absorption can take place between the energy levels of a quantum well associated with the conduction band or the valence band.

QUANTUM WELL INFRARED PHOTODETECTORS (QWIPs)

The idea of using a quantum well to detect light can be understood by the basic principles of quantum mechanics[4]. An electron in a square quantum well is the classic particle-in-a-box of basic quantum mechanics. Such a square quantum well can be created in the lattice-matched $GaAs/Al_xGa_{1-x}As$ material system by sandwiching a layer of GaAs between two layers of $Al_xGa_{1-x}As$. The bandgap of $Al_xGa_{1-x}As$ being larger than that of GaAs, results in a square quantum well for electrons in the conduction band: the GaAs layer is the well layer; the $Al_xGa_{1-x}As$ layers on either side are the potential barriers. The depth of the potential well (= the height of the potential barrier) can be precisely controlled by controlling the Al mole fraction x in the $Al_xGa_{1-x}As$ barrier layers. State-of-the-art crystal growth techniques like molecular beam epitaxy (MBE) permit the epitaxial growth of such layers, typically on a 3-6 inch diameter ~ 600-μm thick GaAs substrate, with ultra-high purity and with control of layer thickness down to a fraction of a molecular layer. This allows the width of the GaAs well layer (one of the design parameters) to be precisely controlled, and the interfaces between the well and barrier layers to be made truly sharp to produce a textbook square quantum well. A controlled number of ground state electrons are provided by doping the GaAs well with Si (an n-type dopant) during the MBE growth. Several quantum wells (sandwiched between barriers) are usually grown stacked on top of each other to increase photon absorption. The upper limit on this number for a typical detector structure in this material system is around 50, about the number of wells and barriers that a photoelectron can traverse in an electric field without being captured by a well downstream from the well which the electron originated. The entire MQW stack is sandwiched between heavily-doped top (called the emitter) and bottom (called the collector) GaAs layers which provide electrical contacts to the device. Absorption of a photon excites an electron from the ground state to the first excited state near the well top, where it can tunnel out to the continuum (continuous energy levels above the quantum well) in the presence of an external voltage bias, thereby producing a photocurrent as shown in Fig. 2.

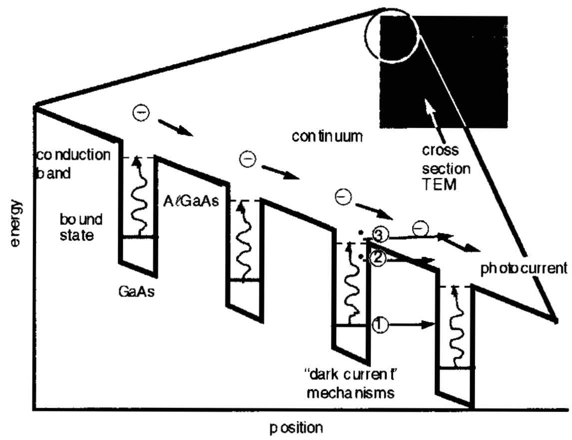

Figure 2 A typical conduction-band diagram of very long wavelength bound-to-continuum quantum well infrared photodetector.

DARK CURRENT REDUCTION (Funded by NASA Office of Space Science)

In addition to the photocurrent, all detectors including QWIPs produce a parasitic current called dark current, which must be minimized to achieve high performance. The dark current is the current flowing through the detector when it is in the dark (i.e. with no photons impinging on it) and is ideally zero. In most applications the *total* current flowing through the detector is measured and there is no way to distinguish the dark current from the photocurrent. Though this dark current can be approximately subtracted in the image-processing electronics, a high dark current implies that the detector blinds itself even when it sees no photons; when it does see photons the image-processing electronics are swamped by the dark electrons with very little capacity left to process the photoelectrons. In QWIPs, the dark current originates from three different mechanisms, as shown in Fig. 2. The dark current arising from the first process is due to quantum mechanical tunneling of ground state electrons from well to well through the $Al_xGa_{1-x}As$ barriers (sequential tunneling). This process is independent of temperature. Sequential tunneling dominates the dark current at very low temperatures (< 30 K). The second mechanism is thermally-assisted tunneling which involves thermal excitation of a ground state electron followed by its tunneling through the tip of the barrier into the continuum energy levels. This process governs the dark current at medium temperatures. The third mechanism is classical thermionic emission (the emission of electrons over a finite potential barrier due to their finite temperature) and dominates the dark current at higher temperatures (> 45 K). Reducing the dark current due to this mechanism is critical to the success of the QWIP since it enables the highly desirable higher temperature camera operation.

Another trick to reduce the dark current due to thermionic emission and optimize the performance of LWIR QWIPs has been devised by Sarath Gunapala *et al.*[4] at JPL, and was sponsored by NASA Office of Space Science. This QWIP uses *bound-to-quasibound* intersubband absorption (occurring when the first excited state is in resonance with the top of the well). This transition maximizes the intersubband absorption while maintaining excellent electron transport. The major advantage of this design lies in the fact that it increases the energy barrier to thermionic emission compared to the case of the bound-to-continuum QWIP (see Fig. 3).

LIGHT COUPLING SCHEMES FOR QWIPs (Funded by NASA Office of Space Science)

In order to be absorbed by the electrons in the quantum wells, the incoming light should have an electric field component in the quantum well direction, i.e., in the growth direction, normal to the layers. Only in this situation is the electric field of the light coupled to the quantized electron momentum, enabling a photon to excite an electron and get absorbed in the process. Light being a transverse wave (whose electric field is perpendicular to the direction of travel), this selection rule means that light striking the layers normally (the most direct way to illuminate an imaging array of detectors) is not absorbed. This clearly limits the configuration of detectors to linear arrays and single elements. For imaging, it is necessary to be able to couple light uniformly to two-dimensional arrays of detectors.

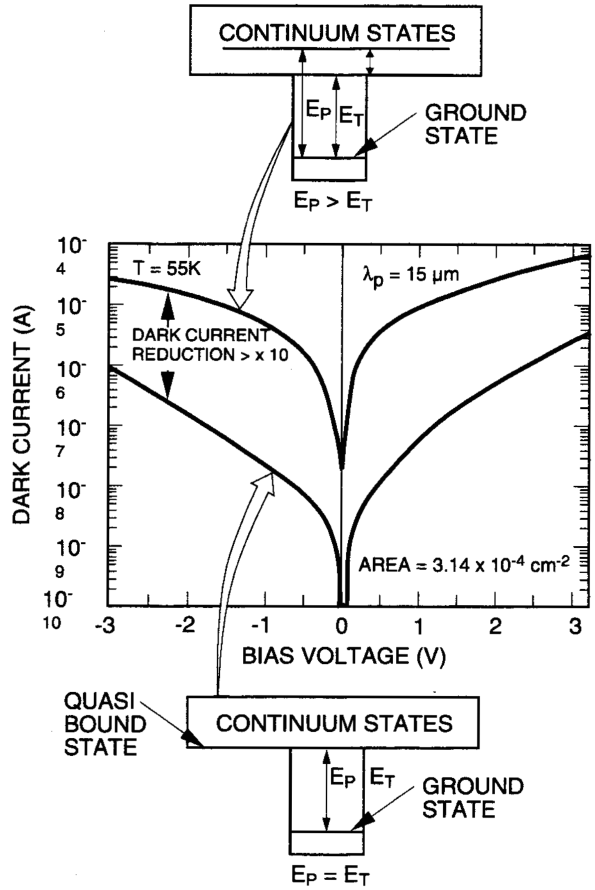

Figure 3. Comparison of dark currents of bound-to-continuum and bound-to-quasibound LWIR QWIPs as a function of bias voltage at temperature T = 70K. Data were taken with a 200 μm diam test structure and normalized to 28x28 μm^2 pixel.

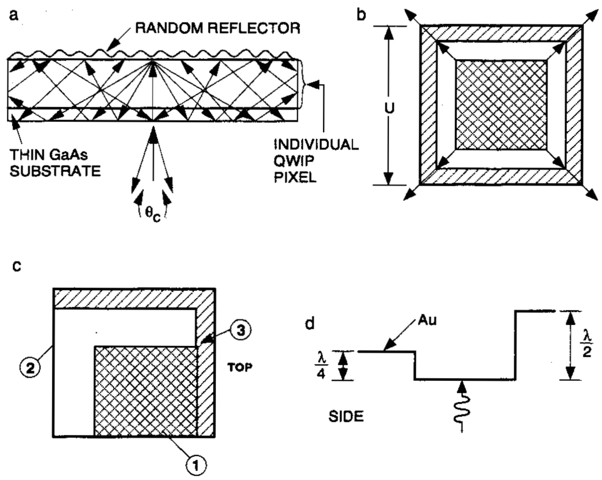

Figure 4. (a) Schematic side view of a thin QWIP pixel with a random reflector. Ideally all the radiation is trapped except for a small fraction which escape through the escape cone (defined by critical angle Θ_c), (b) top view of the unit cell of the scattering surface (arrows indicate the 16 random possibilities), (c) top view of the one of the 16 possibilities, (d) side view of the unit cell (129).

This is accomplished by putting a special reflector on the detector top and illuminating the detector from the back. To be useful, the mirror has to be rough (on the scale of the wavelength of the light in the detector's GaAs material). This roughness may be either periodic or random (see Fig. 4). A rough mirror scatters or sprays the incident light back in a cone (i.e., the roughness ensures that the angle of reflection no longer equals the angle of incidence). The details of the cone depend on the details of the roughness. This cone now strikes the bottom side. Those rays that are within a critical angle of the normal (17° for the GaAs-air interface) refract or escape back into the air. The rest suffer total internal reflection with the back surface acting as a smooth mirror. The internally reflected rays are once again reflected off the top rough mirror. What happens next depends on whether the roughness of the top mirror is periodic or random. If it is periodic, the top mirror will scatter or bend these rays so that they are all normal to the quantum well layers again. These rays pass through the detector and out of the backside. A *randomly* roughened mirror, on the other hand, will randomly reflect or scatter all the rays internally reflected on to it from the bottom side each time, thereby allowing the incident light to bounce back and forth between the detector top and back surfaces several times. Only light within a 17° (from normal) cone escapes out of the backside. Clever design can reduce the amount of light in the escape cone but cannot eliminate it altogether. For instance, if the random reflector is designed with two levels of rough surfaces having the same areas but located a quarter wavelength ($\lambda_{GaAs}/4$) apart, the *normally* reflected light intensities from the top and bottom surfaces of the reflector are equal and 180° out of phase (see Fig. 4). This maximizes the destructive interference at normal reflection and lowers light leakage through the escape cone. The random reflector is fabricated on the QWIPs using standard photolithography and CCl_2F_2 selective dry etching. The advantage of the photolithographic process over a completely random process is the ability to accurately control feature size and preserve the pixel-to-pixel uniformity necessary for very sensitive imaging FPAs. This research was sponsored by NASA Office of Space Science.

DEVELOPMENT OF QWIP IMAGING ARRAYS (Jointly funded by NASA Office of Space Science, BMDO's Innovative Science and Technology Office, and Air Force Research Laboratory)

(A) 128x128 15μm cutoff QWIP Imaging Camera (Funded by NASA Office of Space Science and BMDO's Innovative Science and Technology Office)

The first 15 μm cutoff FPA camera was demonstrated by Gunapala *et al.*,[5] which consisted of bound-to-quasibound QWIPs (funded by NASA Office of Space Science). Four device structures were grown on 3 inch GaAs wafers and each wafer processed into 35 128x128 FPAs. The pixel pitch of the FPA is 50 μm and the actual pixel size is 38x38 μm^2. Two level random reflectors were used to improve the light coupling on top of each pixel. These random reflectors, which were etched to a depth of half a peak wavelength in GaAs using reactive-ion etching, had a square profile. These reflectors are covered with Au/Ge and Au (for Ohmic contact and reflection), and In bumps are evaporated on top for silicon multiplexer hybridization. A single QWIP FPA was chosen (cutoff wavelength of this sample is 14.9 μm) and bonded to a silicon readout multiplexer. FPA was back-illuminated through the flat thinned substrate. This initial array gave excellent images with 99.9% of the pixels working, demonstrating the high yield of GaAs technology. As mentioned earlier this high yield is due to the excellent GaAs growth uniformity and the mature GaAs processing technology. The uniformity after two point correction was u = 0.03%. This research was funded by NASA Office of Space Science, and BMDO's Innovative Science and Technology Office.

(B) 256x256 Hand-held LWIR Imaging Camera (Funded by BMDO's Innovative Science and Technology Office)

The first 256x256 LWIR hand-held imaging camera was demonstrated by Gunapala *et al.*[6]. The device structure of this FPA consisted of a bound-to-quasibound QWIP containing 50 periods of a 45 Å well of GaAs (doped n = 4×10^{17} cm^{-3}) and a 500 Å barrier of $Al_{0.3}Ga_{0.7}As$. After the random reflector array was defined by the lithography and dry etching, the photoconductive QWIPs of the 256x256 FPAs were fabricated by wet chemical etching through the photosensitive $GaAs/Al_xGa_{1-x}As$ MQW layers into the 0.5 μm thick doped GaAs bottom contact layer. The pitch of the FPA is 38 μm and the actual pixel size is 28x28 μm^2. The random reflectors on top of the detectors were then covered with Au/Ge and Au for Ohmic contact and reflection. A single QWIP FPA was chosen and hybridized (via indium bump-bonding process) to a 256x256 CMOS readout multiplexer (Amber AE-166) and biased at V_B = -1.0 V. The FPA was back-illuminated through the flat thinned substrate membrane (thickness ≈ 1300 Å). This initial array gave excellent images with 99.98% of the pixels working (number of dead pixels ≈ 10), demonstrating the high yield of GaAs technology. The measured NEΔT of the FPA at an operating temperature of T = 70 K, bias V_B = -1 V, and for 300 K background is 15 mK. This agrees reasonably with our estimated value of 8 mK based on test structure data. The peak quantum efficiency of the FPA was 3.3% (lower FPA quantum efficiency is attributed to 54% fill factor and 90% charge injection efficiency) and this corresponds to an average of three passes of infrared radiation (equivalent to a single 45° pass) through the photosensitive MQW region.

A 256x256 QWIP FPA hybrid was mounted onto a 250 mW integral Sterling closed-cycle cooler assembly and installed into an Amber RADIANCE 1™ camera-body to demonstrate the hand-held LWIR camera (shown in Fig. 5). The camera is equipped with a 32-bit floating-point digital signal processor combined with multi-tasking software, providing the speed and power to execute complex image-processing and analysis functions inside the camera body itself. The other element of the camera is a 100 mm focal length germanium lens, with a 5.5 degree field of view. It is designed to be transparent in the 8-12 μm wavelength range to be compatible with the QWIP's 8.5 μm operation. This research was funded by BMDO's Innovative Science and Technology Office.

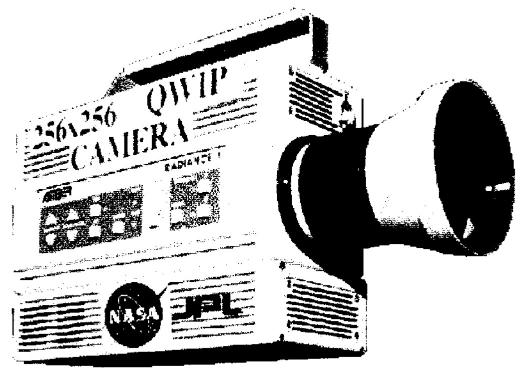

Figure 5. Picture of the first 256 x 256 hand-held long wavelength QWIP camera (QWIP RADIANCE).

(C) 640X486 LWIR Imaging Camera (Funded by NASA Office of Space Science, BMDO's Innovative Science and Technology Office)

After the 2-D grating array was defined by the photolithography and dry etching, the photoconductive QWIPs of the 640x486 FPAs were fabricated[7] by wet chemical etching through the photosensitive $GaAs/Al_xGa_{1-x}As$ multi-quantum well layers into the 0.5 μm thick doped GaAs bottom contact layer. The pitch of the FPA is 25 μm and the actual pixel size is 18x18 μm^2. The cross gratings on top of the detectors were then covered with Au/Ge and Au for Ohmic contact and reflection. A single QWIP FPA was chosen and hybridized to a 640x486 direct injection silicon readout multiplexer (Amber AE-181) and biased at V_B = -2.0 V. The FPA was back- illuminated through the flat thinned substrate membrane (thickness ≈ 1300 Å). This thinned GaAs FPA membrane has completely eliminated the thermal mismatch between the silicon CMOS readout multiplexer and the GaAs based QWIP FPA. Basically, the thinned GaAs based QWIP FPA membrane adapts to the thermal expansion and contraction coefficients of the silicon readout multiplexer. Therefore, this thinning has played an extremely important role in the fabrication of large area FPA hybrids. In addition, this thinning has completely eliminated the pixel-to-pixel optical cross-talk of the FPA. This initial array gave excellent images with 99.9% of the pixels working, demonstrating the high yield of GaAs technology. The experimentally measured NEΔT of the FPA is 36 mK at an operating temperature of T = 70 K, bias V_B = -2 V, and at 300 K background. This agrees reasonably with our estimated value of 25mK based on test structure data. The experimentally measured peak quantum efficiency of the FPA was 2.3% (lower focal plane array quantum efficiency is attributed to 51% fill factor and 30% reflection loss from the GaAs back surface). Therefore, the corrected quantum efficiency of focal plane detectors is 6.5% and this corresponds to an average of two passes of IR radiation (equivalent to a single 45° pass) through the photosensitive MQW region.

A 640X486 QWIP FPA hybrid was mounted onto a 84-pin lead-less chip carrier and installed into a laboratory dewar which is cooled by liquid nitrogen (to demonstrate a LWIR imaging camera). The other element of the camera is a 100 mm focal length AR coated germanium lens, which gives a 9.2°x6.9° field of view. The uncorrected NEΔT non-uniformity of the 640x486 FPA is about 5.6% (= sigma/ mean).

Video images were taken at a frame rate of 30 Hz at temperatures as high as T = 70 K using a ROC capacitor having a charge capacity of 9×10^6 electrons. The non-uniformity after two-point (17° and 27° Celsius) correction improves to an impressive 0.1%. Figure 6 shows a frame of a video image taken with this long-wavelength 640x486 QWIP camera. This image demonstrates the high sensitivity of the 640 x 486 long-wavelength QWIP staring array camera. As mentioned earlier, this high yield is due to the excellent GaAs growth uniformity and the mature GaAs processing technology. This research was funded by NASA Office of Space Science, BMDO's Innovative Science and Technology Office.

Figure 6. This picture was taken in the night (around midnight) and it clearly shows where automobiles were parked during the day time. This image demonstrates the high sensitivity of the 640 x 486 long-wavelength QWIP staring array camera.

(D) Broad-band QWIP (Funded by NASA Office of Space Science)

A broad-band MQW structure can be designed by repeating a unit of several quantum wells with slightly different parameters such as well width and barrier height. The device structure involved 33 repeated layers of GaAs three-quantum-well units separated by L_B ~ 575 Å thick $Al_xGa_{1-x}As$ barriers [8]. The well thickness of the quantum wells of three-quantum-well units are designed to respond at peak wavelengths around 13, 14, and 15μm respectively. These wells are separated by L_u ~ 75 Å thick $Al_xGa_{1-x}As$ barriers. The Al mole fraction (x) of barriers throughout the structure was chosen such that the λ_p = 13 μm quantum well operates under bound-to-quasibound conditions. The excited state energy level broadening is further enhanced due to overlap of the wavefunctions associated with excited states of quantum wells separated by thin barriers. Energy band calculations based on a two band model shows excited state energy levels spreading about 28 meV. The detectors were back illuminated through a 45° polished facet to obtain normalized responsivity spectra at different bias voltages. Then the absolute spectral responsivities were obtained by measuring total photocurrent from a calibrated blackbody source. In Fig. 7, responsivity curve at V_B = -3 V bias voltage shows broadening of the spectral response up to Δλ ~ 5.5 μm, i.e. the full width at half maximum from 10.5 - 16μm.

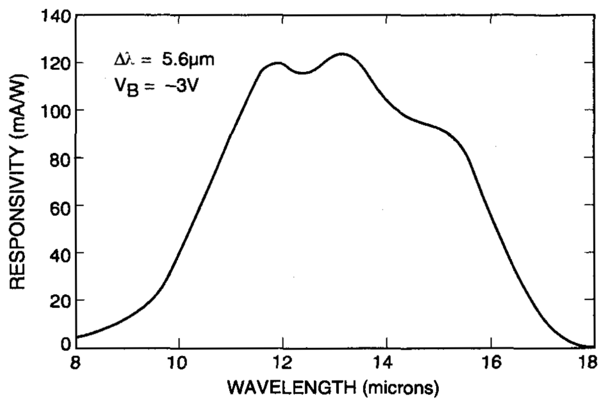

Figure 7. Experimentally measured responsivity spectrum of broadband QWIP at bias voltage V_B=-3 V.

This broadening $\Delta\lambda/\lambda_p \sim 42$ % is about a 400 % increase compared to a typical bound-to-quasibound QWIP.

(E) Dualband Detectors (Funded by Air Force Research Laboratory)

There are several applications such as target recognition and discrimination which require monolithic mid-, long-wavelength and -very-long-wavelength dualband large area, uniform, reproducible, low cost and low 1/f noise infrared FPAs. For example, a dualband FPA camera would provide the absolute temperature of the target, which is extremely important to the process of identifying temperature difference between targets, warheads and decoys. The GaAs based QWIP is a potential candidate for development of such a two-color FPAs.

Gunapala *et al.*[9] have developed a two-color, two stack, QWIP device structure based on $In_xGa_{1-x}As/Al_yGa_{1-y}As/GaAs$ material system for MWIR/LWIR and LWIR/VLWIR detection. This structure can be processed in to dualband QWIP FPAs with dual or triple contacts to access the CMOS readout multiplexer. The device structure consists of a stack of 25 periods of LWIR QWIP structure and another stack of 25 periods of VLWIR QWIP structure separated by a heavily doped 0.5 μm thick intermediate GaAs contact layer. The first stack (VLWIR) consists of 25 periods of 500 Å $Al_xGa_{1-x}As$ barrier and a GaAs well. This VLWIR QWIP structure has been designed to have a bound-to-quasibound intersubband absorption peak at 15 μm, since the dark current of the device structure is expected to be dominated by the longer wavelength portion of the device structure. The second stack (LWIR) consists of 25 periods of 500 Å $Al_xGa_{1-x}As$ barrier and a narrow GaAs well. This LWIR QWIP structure has been designed to have a bound-to-continuum intersubband absorption peak at 8.5 μm, since photocurrent and dark current of the LWIR device structure are relatively small compared to the VLWIR portion of the device structure. This whole dualband QWIP structure is then sandwiched between 0.5 μm GaAs top and bottom contact layers doped n = 5 x 10^{17} cm^{-3}, and has been grown on a semi-insulating GaAs substrate by MBE. Then a 1.0 μm thick GaAs cap layer on top of a 300 Å $Al_{0.3}Ga_{0.7}As$ stop-etch layer has to be grown in situ on top of the device structure for the fabrication of a light coupling optical cavity. The peak detectivities D^*_λ of LWIR and VLWIR detectors were 1.8 x 10^{12} cm $\sqrt{Hz}$/W (at T = 55K and V_B = 1.0) and 1.5 x 10^{12} cm$\sqrt{Hz}$/W (at T = 35K and V_B = 1.0) respectively. This research will lead to development of hyper spectral FPAs for NASA Space Science and Earth Science applications.

(F) High Performance QWIPs for Low Background Applications (Funded by NASA Office of Space Science and Air Force Research Laboratory)

In this section, we discuss the demonstration of high performance QWIPs for low background applications by Gunapala *et al.*[9]. Improving QWIP performance depends largely on minimizing the Shott noise of the dark and improving the quantum efficiency. In order to analyze the dark current of a QWIP which has a intersubband absorption peak in the long-wavelength region, we first calculated the effective number of electrons[4] n(V) which are thermally excited into the continuum transport states, as a function of bias voltage V. Eight n-type doped QWIP device structures were grown for this experiment. All eight QWIP samples were processed into 200 μm diameter mesas (area = 3.14 x 10^{-4} cm^2) using wet chemical etching and Au/Ge ohmic contacts were evaporated onto the top and bottom contact layers.

The responsivities of all device structures peaked in the range from 7.7 μm to 9.7 μm. It is worth noting that ηg product of 17% is achieved. This is approximately a factor of 24 increase in hg product compared to ηg product of our QWIP devices designed for high background and high temperature operation. These detectors show background limited performance (BLIP) for moderately low background of 2 x 10^9 photons/cm^2/sec at T = 40 K operation. Since the dark current of these detectors is thermionically limited down to T = 30 K, these detectors should demonstrated a BLIP at T = 35 K for 2 x 10^9 photons/cm^2/sec background. These results will lead to the development of high-performance QWIP FPAs for Palomar 200-inch Hale telescope and development of high-performance QWIP FPAs for Air Force strategic applications. This is a very good example of how interagency funding can help NASA's Space Science program.

APPLICATIONS

(A) Outreach (NASA)

As part of the NASA outreach program, we have brought our research achievements to some of our local schools. The asset of this nation is our young people, especially while they are in their most impressionable ages. Introducing them to our current technology and how it relates to science and technology will hopefully spark an interest in their minds. Perhaps these young minds will one day be the people to push the frontier of science and technology to new levels.

We had the opportunity to take our QWIP camera to Meadows Elementary school's sixth grade classes. As part of their curriculum, they are learning about the formation of the universe and to identify different celestial objects. During our demonstration, we showed the students how scientists today study the universe by examining the various segments of the electromagnetic spectrum using existing technology. We utilized a simple optical setup we fabricated to show the sixth grade students how different wavelengths of light can be separated. We also used the QWIP infrared camera to show what a different and interesting world exists beyond visible wavelength, and how each bit of information in different segments of the electromagnetic spectrum helps scientists to see a larger picture of our universe.

(B) Spatial Fourier Transform Imaging Spectrometer (NASA Space Science and Earth Science)

In FY'98 JPL technologist Francis Reininger built a prototype point spectrometer called the Spatially Modulated Infrared Spectrograph (SMIS) based on the 640x486 LWIR QWIP camera which was Jointly funded by NASA Office of Space Science, and BMDO's Innovative Science and Technology Office. SMIS is a special interferometer that can instantaneously convert an input beam into a white light fringe pattern along a detector FPA without any moving parts. The large uniform QWIP FPA camera is a key element in SMIS, because, the beam is spatially modulated or divided along a large uniform detector array into spatial bins of white light. Study of the data collected from SMIS based on JPL's new 640x486 LWIR QWIP camera indicates that it could map hydrothermal vents and water vapor sources on Mars and meet the 15 kg payload limit for micro-missions to Mars. One or the most unique characteristic of this instrument (besides being small and efficient) is that it has one instrument line shape for all spectral colors and spatial field positions. By using broad-band QWIP arrays with wavelengths out to 16 μm, the next version of this instrument could become the first compact, high-resolution thermal infrared, hyper-spectral imager with a single spectral line shape and zero spectral smile. Such an instrument is in strong demand by scientists studying Earth and planetary science. This is another classic example of how interagency technology collaborations could help NASA Earth and space science programs.

(C) Astronomy (NASA Space Science)

In this section, we discuss the first astronomical observations with a QWIP FPA. In order to perform this astronomical observation, we designed a QWIP wide-field imaging multi-color prime-focus infrared camera (QWICPIC). Observations were conducted at the five meter Hale telescope at Mt. Palomar with QWICPIC based on 8-9 μm 256x256 QWIP FPA operating at T=35 K. The ability of QWIPs to operate under high photon backgrounds without excess noise enables the instrument to observe from the prime focus with a wide 2'x2' field of view, making this camera unique among the suite of IR instruments available for astronomy. The excellent 1/f noise performance of QWIP FPAs allows QWICPIC to observe in a slow scan strategy often required in infrared observations from space[9].

Figure 9 compares an image of the Orion nebula obtained in a brief 30 minute observation with an engineering grade QWIP FPA to a visible image of the Orion nebula taken with the wide field planetary camera in Hubble Space Telescope (HST). In addition to the well-known IR bright BN-KL object in the upper right-hand corner, careful comparison of the IR images with optical and near-IR images obtained by HST reveal a multitude of IR sources which are dim or undetectable in visible. These images demonstrate the advantage of large format, stable (low 1/f noise) LWIR QWIP FPAs for surveying obscured regions in search for embedded or reddened objects such as young forming stars.

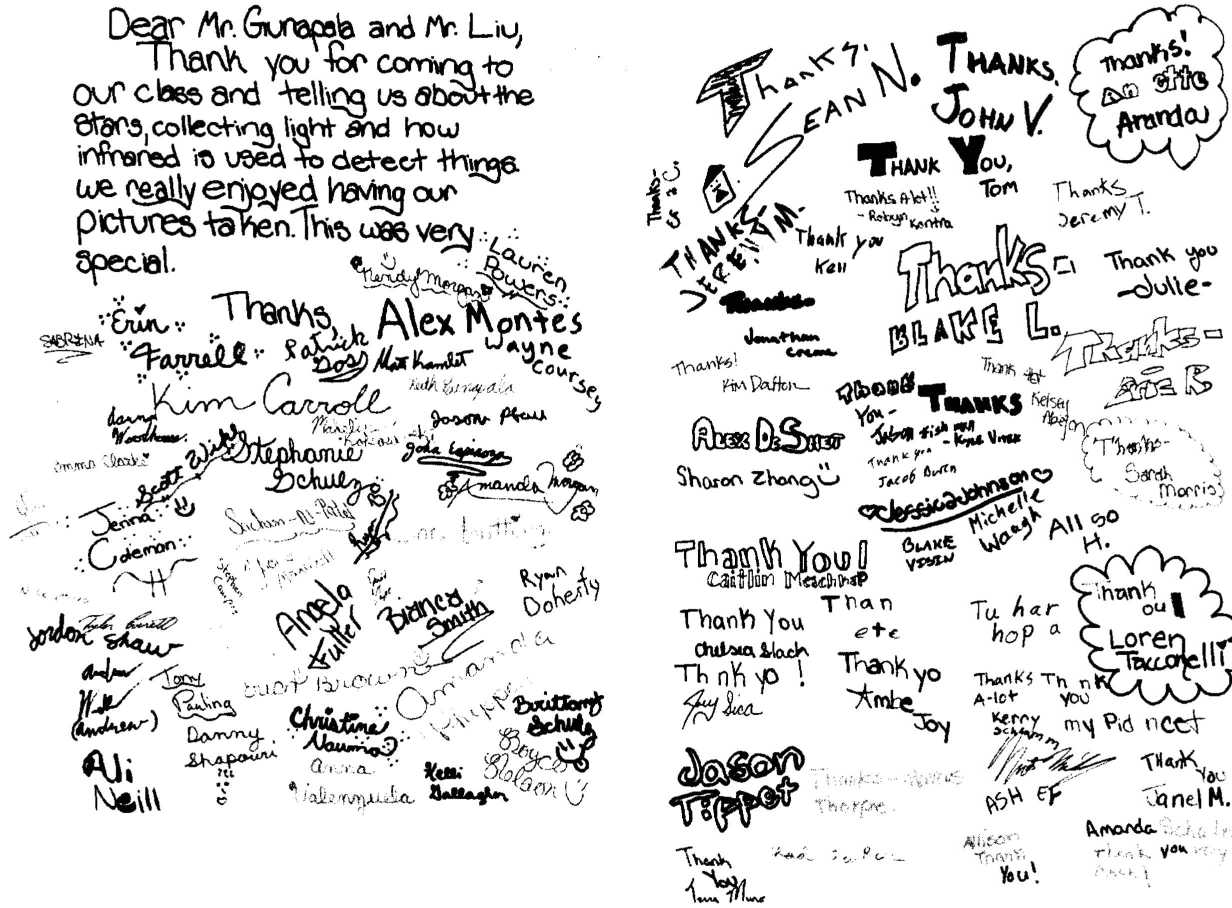

Figure 8. Image of the thanking card sent by sixth grader's of Meadows Elementary School Newhall School District, Valencia, CA

(D) Fire Fighting (Department of Interior)

Recently, 256 x 256 format hand-held QWIP cameras have been used to demonstrate various applications in science, medicine, industry, defense, etc. A 256 x 256 portable LWIR QWIP camera helped a Los Angeles TV news crew get a unique perspective on fires that raced through the Southern California seaside community of Malibu in October, 1996. The camera was used on the station's news helicopter. This portable camera features IR detectors which cover longer wavelengths than previous portable cameras could. This allows the camera to see through smoke and pinpoint lingering hotspots, which are not normally visible. This enabled the TV station to transmit live images of hotspots, which appeared innocuous to the naked eye. These hotspots were a source of concern and difficulty for firefighters, because they could flare up even after the fire appeared to have subsided. Figure 10 shows the comparison of visible and infrared images of a just burned area as seen by the news crew in nighttime. It works effectively in both daylight and nighttime conditions. The event marked the QWIP camera's debut as a fire observing device[9].

(E) Volcanology (NASA Earth Science)

A similar 256 x 256 format LWIR QWIP camera has been used to observe volcanoes, mineral formations, weather and atmospheric conditions at the Kilauea Volcano, Hawaii. The objectives of this trip were to map geothermal features. The wide dynamic range enabled volcanologists to image volcanic features at temperatures much higher (300 - 1000 C) than can be imaged with conventional thermal imaging systems in the 3 - 5 μm range or in visible. Figure 11 shows the comparison of visible and IR images of the Kilauea Volcano in Hawaii. The IR image of the volcano clearly shows a hot lava tube running underground which is not visible to the naked eye.

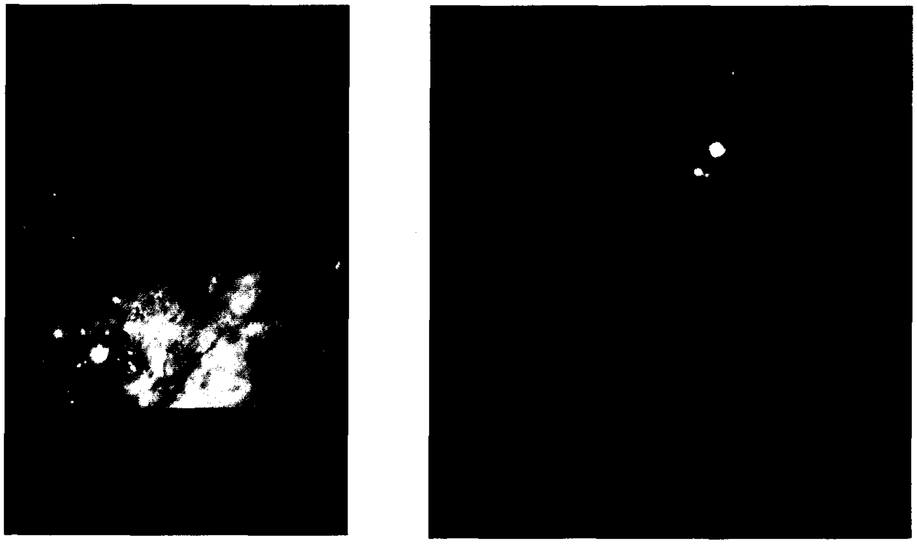

(a) (b)

Figure 9. Visible image of the Orion nebula taken with the wide field planetary camera in Hubble Space Telescope. (b) 8-9 μm infrared image of the Orion nebula taken with an engineering grade 256 x 256 QWIP FAA at five meter Hale telescope at Mt. Palomar.

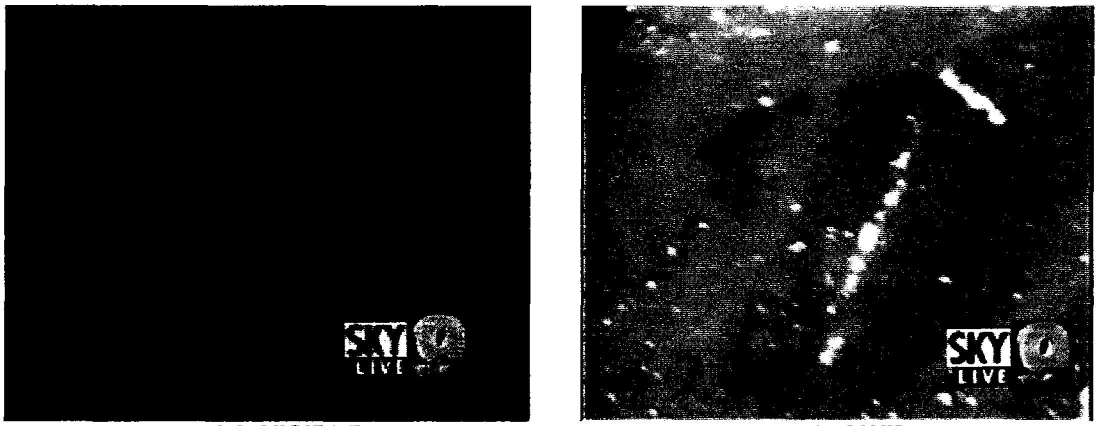

(a) VISIBLE **(b) QWIP**

Figure 10. Comparison of visible and infrared images of a just burned area as seen by a highly sensitive visible CCD camera and the long wavelength infrared camera in nighttime. (a) Visible image from a CCD camera. (b) Image from the 256 x 256 portable QWIP camera. This portable camera features infrared detectors which covers longer wavelengths than previous portable cameras could. This allows the camera to see through smoke and pinpoint lingering hotspots which are not normally visible. This enables firefighters to locate the hotspots in areas which appeared innocuous to the naked eye. These hotspots are a source of concern and difficult for firefighters, because they can flare up even after the fire appears to have subsided. It works effectively in both daylight and nighttime conditions.

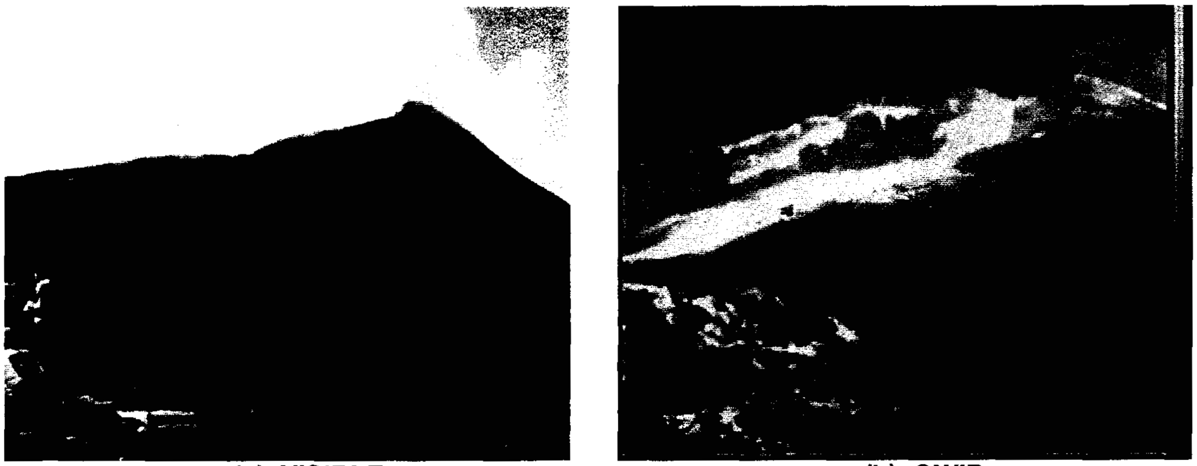

Figure 11. Comparison of visible and infrared images of the Mount Kilauea Volcano in Hawaii. (a) Visible image from a highly sensitive CCD camera. (b) Image from the 256 x 256 portable QWIP camera. The wide dynamic range enabled us to image volcanic features at temperatures much higher (300-1000C) than can be imaged with conventional thermal imaging systems in the 3-5 μm range or in visible. The infrared image of the volcano clearly shows a hot lava tube running underground which is not visible to the naked eye. This demonstrates the advantages of long wavelength infrared in geothermal mapping.

(F) Medicine (Public Outreach)

A group of researchers from the State University of New York in Buffalo and Walter Reed Army Institute of Research in Washington DC have used it in Dynamic Area Telethermometry (DAT). DAT has been used to study the physiology and patho-physiology of cutaneous perfusion, which has many clinical applications. DAT involves accumulation of hundreds of consecutive IR images and fast Fourier transform (FFT) analysis of the biomodulation of skin temperature, and of the microhomogeneity of skin temperature (HST, which measures the perfusion of the skin's capillaries). The FFT analysis yields the thermoregulatory frequencies and amplitudes of temperature and HST modulation. To obtain reliable DAT data, one needs an IR camera in the >8 μm range (to avoid artifacts of reflections of modulated emitters in the environment), a repetition rate of 30 Hz (allowing accumulation of a maximal number of images during the observation period to maximize the resolution of the FFT), frame to frame instrumental stability (to avoid artifact stemming from instrument modulation), and sensitivity of less than 50 mK. According to these researchers, the longer wavelength operation, higher spatial resolution, higher sensitivity, and greater stability of the QWIP RADIANCE made it the best choice of all IR cameras.

This camera has also been used by a group of researchers at the Texas Heart Institute in a heart surgery experiment performed on a rabbit heart. This experiment clearly revealed that it is possible to detect arterial plaque built inside a heart by thermography. Figure 12 clearly shows arterial plaque accumulated in a rabbit heart.

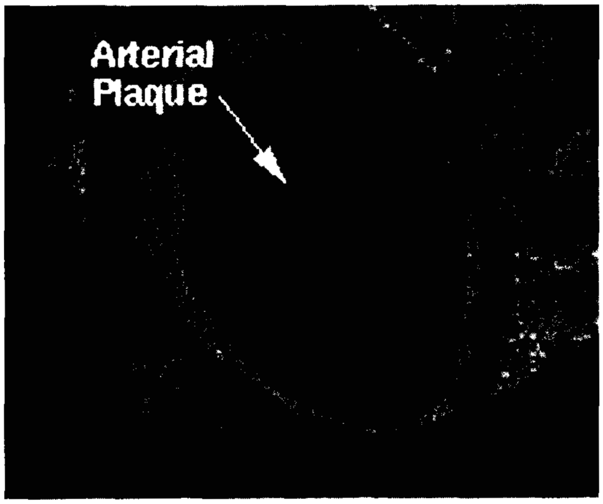

Figure 12. This image shows arterial plaque deposited in a rabbit heart.

(G) Defense (BMDO)

It is not necessary to explain how real time IR imaging is important in surveillance, reconnaissance and military operations. The QWIP RADIANCE was used by the researchers at BMDO's innovative science and technology experimental facility in a unique experiment to discriminate and clearly identify the cold launch vehicle from its hot plume emanating from rocket engines.

Usually, the temperature of cold launch vehicles is about 250°C, whereas the temperatures of the hot plume emanating from launch vehicle can reach 950°C. According to the Plank's blackbody emission theory, the photon flux ratio between 250°C and 950°C blackbodies at 4 μm is about 25,000, whereas the same photon flux ratio at 8.5 μm is about 115. Thus, it is very clear that one must explore longer wavelengths for better cold-body versus hot plume discrimination[9], because the highest instantaneous dynamic range of infrared cameras is usually 12-bits (i.e., 4096) or less. Figure 13 shows an image of Delta-II launch taken with QWIP RADIANCE camera. This clearly indicates the advantage of long-wavelength QWIP cameras in the discrimination and identification of cold launch vehicles in the presence of a hot plume during early stages of launch.

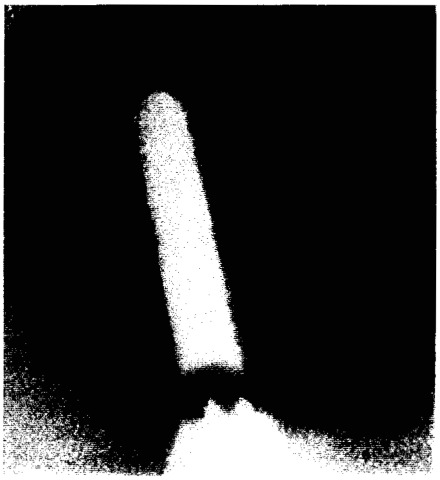

Figure 13. Image of a Delta-II launch vehicle taken with the long-wavelength QWIP RADIANCE during the launch. This clearly indicates the advantage of long-wavelength QWIP cameras in the discrimination and identification of cold launch vehicles in the presence of hot plume during early stages of launch.

SUMMARY

As a result of interagency technology partnering, exceptionally rapid progress has been made in the development of long-wavelength QWIPs, since they were first experimentally demonstrated several years ago. It is now possible for QWIPs to achieve excellent performance (e.g., detectivities as high as $D^* \sim 1\times10^{11}$ cm$\sqrt{\text{Hz}}$/W at 70 K for a 9 μm QWIP) and be fabricated into large inexpensive low-noise imaging arrays. A 70 K operating temperature can be easily achieved by single-stage Stirling cycle coolers, which allowed us to demonstrate the first palm-size 256x256 FPA LWIR camera based on QWIPs. Weighing about 2.5 pounds, the QWIP InfraCam is entirely self-contained, with no extra boxes for control, cooling, or image processing. Its sharp, inexpensive, large, uniform, infrared eye (which can be tailored to see a particular IR wavelength) makes the QWIP palm-size camera the best and the most cost-effective new tool for imaging and spectroscopy for NASA's faster, better, cheaper Earth and Space Science programs. This a classic example how effective partnering of government agencies and industries can help further the scope of NASA Space Science and Earth Science programs, advancement of technology, education, and outreach.

ACKNOWLEDGMENTS

The research described in this paper was performed by the Center for Space Microelectronics Technology, Jet Propulsion Laboratory, California Institute of Technology, and was jointly sponsored by the National Aeronautics and Space Administration Office of Space Science, the Ballistic Missile Defense Organization / Innovative Science & Technology Office, Air Force Research Laboratory, and JPL Director's Research and Development Fund.

REFERENCES

1. M. T. Chahine, Proceedings of Innovative Long Wavelength Infrared Detector Workshop, Pasadena, California, April 24-26, 1990.
2. Duston, "BMDO's IS&T faces new hi-tech priorities", *BMD Monitor*, pp 180-183, May 19, 1995.
3. F. Levine, J. Appl. Phys. **74**, R1 (1993).
4. D. Gunapala and K. M. S. V. Bandara, Physics of Thin Films, Academic Press, **21**, 113 (1995).
5. Sarath D. Gunapala, John K. Liu, Jin S. Park, Mani Sundaram, Craig A. Shott, Ted Hoelter, True-Lon Lin, S. T. Massie, Paul D. Maker, Richard E. Muller, and Gabby Sarusi" 9 μm Cutoff 256x256 $GaAs/Al_xGa_{1-x}As$ Quantum Well Infrared Photodetector Hand-Held Camera", IEEE Trans. Electron Devices, **44**, pp. 51-57, 1997.
6. Sarath D. Gunapala, Jin S. Park, Gabby Sarusi, True-Lon. Lin, John K. Liu, Paul D. Maker, Richard E. Muller, Craig A. Shott, and Ted Hoelter, "15 μm 128x128 GaAs/AlGaAs Quantum Well Infrared Photodetector Focal Plane Array Camera", IEEE Trans. Electron Devices, **44**, pp. 45-50, 1997.
7. Sarath D. Gunapala, Sumith V. Bandara, John K. Liu, Winn Hong, Mani Sundaram, Paul D. Maker, Richard E. Muller, Craig A. Shott, and Ronald CarralejoLong-Wavelength 640x486 $GaAs/Al_xGa_{1-x}As$ Quantum Well Infrared Photodetector Snap-shot Camera", IEEE Trans. Electron Devices, **45**, pp. 1890-1895, 1998.
8. V. Bandara, S. D. Gunapala, J. K. Liu, E. M. Mumolo, W. Hong, D. K. Sengupta, and M. J. McKelvey, Appl. Phys. Lett., **72** 2427, 1998.
9. D. Gunapala, S. V. Bandara, J. K. Liu, W. Hong, E. M. Luong, J. M. Mumolo, M. J. McKelvey, D. K. Sengupta, A. Singh, C. A. Shott, R. Carralejo, P. D. Maker, J. J. Bock, M. E. Ressler, M. W. Werner, and T. N. Krabach, "Quantum Well Infrared Photodetectors Research and Development at Jet Propulsion Laboratory", SPIE Proceeding, Infrared Detectors and Focal Plane Arrays V, pp. 382-395, Vol. 3379, 1998.